Oleoylethanolamide mitigates cardiometabolic disruption secondary to obesity induced by high-fat diet in mice

Federica Comella [a], Alana Aragón-Herrera [b,c], Claudio Pirozzi [a], Sandra Feijóo-Bandin [b,c], Adriano Lama [a], Nicola Opallo [a], Stefania Melini [a], Filomena Del Piano [d], Oreste Gualillo [e,f], Rosaria Meli [a], Giuseppina Mattace Raso [a,*,1], Francisca Lago [b,c,**,1]

[a] *Department of Pharmacy, School of Medicine, University of Naples Federico II, 80131 Naples, Italy*
[b] *Cellular and Molecular Cardiology Research Unit, Institute of Biomedical Research of Santiago de Compostela (IDIS), Hospital Clínico Universitario de Santiago de Compostela, Área Sanitaria de Santiago de Compostela y Barbanza (SERGAS), Santiago de Compostela, Spain*
[c] *Centro de Investigación Biomédica en Red de Enfermedades Cardiovasculares (CIBERCV), Instituto de Salud Carlos III, Madrid, Spain*
[d] *Department of Veterinary Medicine and Animal Productions, University of Naples "Federico II, 80100 Naples, Italy*
[e] *SERGAS (Servizo Galego de Saude) and IDIS (Instituto de Investigación Sanitaria de Santiago), The NEIRID Group (Neuroendocrine Interactions in Rheumatology and Inflammatory Diseases), Santiago University Clinical Hospital, Building C, Travesía da Choupana SIN, Santiago de Compostela 15706, Spain*
[f] *International PhD School, University of Santiago de Compostela (EDIUS), Santiago de Compostela 15706, Spain*

A R T I C L E   I N F O

A B S T R A C T

Chronic lipid overnutrition has been demonstrated to promote cardiac dysfunction resulting from metabolic derangement, inflammation, and fibrosis. Oleoylethanolamide (OEA), an endogenous peroxisome proliferator activating receptor (PPAR)-α agonist, has been extensively studied for its metabolic properties.

The aim of this study was to determine if OEA has beneficial effects on high-fat diet (HFD)-induced cardiac disruption in obese mice, focusing on the underlying pathological mechanisms.

OEA treatment restores the metabolic pattern, improving serum glycaemic and lipid profile. OEA also reduces heart weight and serum creatine kinase-myocardial band (CK-MB), a marker of cardiac damage. Accordingly, OEA modulates cardiac metabolism, increasing insulin signaling and reducing lipid accumulation. OEA increases AMPK and AKT phosphorylation, converging in the rise of AS160 activation and glucose transporter (GLUT)4 protein level. Moreover, OEA reduces the transcription of the cardiac fatty acid transporter CD36 and fatty acid synthase and increases PPAR-α mRNA levels. Adiponectin and meteorite-like protein transcription levels were significantly reduced by OEA in HFD mice, as well as those of inflammatory cytokines and pro-fibrotic markers. An increased autophagic process was also shown, contributing to OEA's cardioprotective effects. Metabolomic analyses of cardiac tissue revealed the modulation of different lipids, including triglycerides, glycerophospholipids and sphingomyelins by OEA treatment. In vitro experiments on HL-1 cardiomyocytes showed OEA's capability in reducing inflammation and fibrosis following palmitate challenge, demonstrating a direct activity of OEA on cardiac cells, mainly mediated by PPAR-α activation.

Our results indicate OEA as a potential therapeutic to restrain cardiac damage associated with metabolic disorders.

1. Introduction

Obesity has been recently defined as a heterogeneous entity, often associated with cardiometabolic risk mediators/comorbidities, such as glucose intolerance and type 2 diabetes, hypertension, dyslipidemia, and metainflammation, considered prevalent drivers of increased cardiovascular outcomes [1]. Obesity-associated cardiomyopathy has been related to several detrimental mechanisms, which arise with ongoing overnutrition and weight gain, involving metabolic, hormonal, inflammatory and hemodynamic alterations, finally impacting heart metabolism and function [2,3]. Long-term obesity is accompanied by excessive adipose tissue, and when the storage capacity of adipocytes is exceeded, ectopic fat deposition occurs in physiologically lean tissues, including the heart, leading to an over-reliance on fatty acid accumulation and lipotoxicity [1].

The adult heart constantly generates ATP to maintain contractile function from mitochondrial oxidative phosphorylation (using mainly fatty acids, followed by pyruvate, ketone bodies and amino acids), which contributes to ~95 % of myocardial ATP requirements, and glycolysis, which supplies the remaining 5 % [4]. However, the heart is metabolically flexible, switching between different energy substrates in response to variations in metabolic demand in physiological and pathological conditions to maintain ATP production [5]. Originally, it has been described that the failing heart becomes energy deficient due to metabolic inflexibility and a reduction of mitochondrial oxidative metabolism, which triggers a compensatory shift in the preference of energy substrates, inducing glycolysis, decreasing fatty acid oxidation, and increasing ketone body oxidation [6]. However, the energy metabolic changes that occur in the heart are complex and poorly understood, and nowadays, they are suggested to depend not only on the severity and type of injury but also on the presence of co-morbidities [4]. For example, when heart failure is concomitant with diabetes and obesity, myocardial fatty acid oxidation is increased, while the opposite is observed in heart failure in the presence of hypertension or ischemia [4,7].

Changes in the myocardial microenvironment affect the phenotype of non-cardiomyocytes, i.e. immune cells, playing a pivotal role in cardiac function under both physiological and pathological conditions. The persistent inflammatory process elicited by immune cells could lead to chronic cardiac inflammation, resulting in the secretion of inflammatory factors, including IL-6, IL-1β, and TNF-α, that may exacerbate cardiac injury. It has been demonstrated that long-term exposure to a high-fat diet could lead to the development and progression of fibrosis both in the liver and in the heart [8,9]. The fibrotic process, as the result of a pathological collagen accumulation in the muscle fibers [10,11], is associated with nearly all forms of heart failure, contributing to cardiac dysfunction.

Oleoylethanolamide (OEA), a member of the N-acylethanolamine family, is a natural bioactive monounsaturated lipid involved in several physiological mechanisms related to energy balance [12,13]. OEA has been indicated as a promising therapeutic in obesity and obesity-related diseases due to its capability to decrease food intake and body weight and to enhance satiety and energy expenditure through its high-affinity binding to peroxisome proliferator-activated-receptor (PPAR)-α in rodents and humans [13,14]. Beyond PPAR-α, OEA also binds, although with a lower affinity, to transient receptor potential vanilloid (TRPV)1, being a medium-potency agonist [15]. Notably, OEA counteracts dyslipidemia in obese rats [16] and restores glucose homeostasis, attenuating hyperglycemia in type 2 diabetic mice [17]. Moreover, apart its metabolic effects, OEA also exerts damping effects on inflammation and oxidative stress [18–20]. Interestingly, OEA has been shown to exhibit a cardioprotective effect through multiple mechanisms, being able to attenuate cardiac oxidative stress and cell apoptosis in doxorubicin-injured mice and in HL-1 atrial cardiomyocytes [21] to stimulate fatty acid oxidation [22] and to modulate the excitability and membrane currents of cardiomyocytes [23–25]. Considering the effects of OEA in regulating energy homeostasis and in preserving cardiac function and based on the tight relationship between obesity and the development of cardiovascular disease [26], we hypothesized that OEA could hold the potential for the treatment of cardiometabolic diseases. Therefore, we aimed to investigate whether OEA could target the multiple detrimental mechanisms underlying cardiac disruption associated with metabolic dysfunction in vivo and in vitro, using a model of high-fat diet-induced obesity in mice and palmitate-challenged HL-1 cardiac muscle cell line, respectively.

2. Methods

2.1. Ethical statement

Animal care and experimental procedures were carried out in compliance with International and National Law and Policies and approved by the Local Animal Care Office (Centro Servizi Veterinari, Università degli Studi di Napoli, Federico II, ITA) and the Italian Ministry of Health under protocol no. 1210/2020-PR. Animal studies were performed in compliance with the Italian D.L. (No. 26 of 4 March 2014) of the Italian Ministry of Health and the EU Directive 2010/63/EU for animal experiments, ARRIVE guidelines, and the Basel declaration, including the 3Rs concept.

2.2. Animals and treatments

In this study, we employed 6-week-old male C57Bl/6 J mice (Charles River, Wilmington, MA, USA) maintained with ad libitum access to a standard chow diet and tap water. The standard chow diet had 17 % fat without sucrose, while HFD had 45 % energy derived from fat and 7 % sucrose (D12451, Research diet, USA). The animals were randomly assigned to three different groups ($n = 10$) as reported below: (i) control group (STD) receiving chow standard diet and vehicle (water/PEG/TWEEN 80 (90/5/5 v/v)); (ii) HFD group receiving vehicle; (iii) HFD group treated with OEA (HFD + OEA) at a dose of 2,5 mg/kg/die i.p. (OEA (PubChem CID:5283453) was synthesized in the laboratory). OEA was resuspended in water/PEG/TWEEN 80 (90/5/5 v/v). Treatments started upon 12 weeks of HFD feeding and lasted 8 weeks along with the HFD. The body weight of animals from all groups was evaluated weekly throughout treatment. At the end of the experiment, all mice were anaesthetized with enflurane by inhalation and euthanized, followed by cervical dislocation. Blood and the heart were collected, snap-frozen and stored at −80 °C for subsequent analysis.

2.3. Metabolic cages

Metabolic cages for mice (41700–003, Ugo Basile, ITA) were used to monitor diet intake. Food intake was manually measured at the end of the 8th week of treatment over a period of 24 h and was expressed in kilojoules, considering that the standard diet contained 15,8 Kj/g while the HFD was 21,9 Kj/g.

2.4. Body composition

Body weight was assessed weekly throughout the experimental period. At the end of the 8th week of treatment, before killing, bioelectrical Impedance Analysis (BIA) was performed to evaluate fat body composition using a BIA 101 analyzer modified for the mouse (Akern, ITA). Fat mass content was derived from the difference between body weight and fat-free mass.

2.5. Oral glucose tolerance test

Oral glucose tolerance test (OGTT) was performed on different subgroups of mice (8 animals/each group) at the beginning of the 8th week of OEA treatment. Mice were fasted overnight (12 h), and glycaemia was

measured before glucose challenge and upon glucose solution (1 g/kg) administration (30, 60, 90, and 120 min). During this test, mice had free access to drinking water. Blood glucose levels were determined using the glucometer One Touch Ultrasmart (Lifescan, USA). The area under the curve (AUC) related to glucose level during the time was calculated from time 0 as an integrated and cumulative measure of glycemia up to 120 min for all animals.

2.6. Serum analysis

Serum creatine kinase-myocardial band (CK-MB) level was measured by using a colorimetric assay kit (cat. MAK116, Sigma-Aldrich, USA). The results were expressed using this calculation:

$$CK \ Activity \ (units/L) = (A340) \ final–(A340) \ initial \\ \times 150/(A340) \ calibrator–(A340) \ blank$$

Cholesterol level was measured using a commercially available kit according to the manufacturer's instructions (SGM Italia, Italy and Randox Laboratories ltd., United Kingdom).

2.7. Lipidomic profile of heart tissue

The heart lipidome profiling from STD, HFD and HFD + OEA mice was performed by OWL Metabolomics SL by Rubió (Bizkaia, ES). In brief, Ultra-High Performance Liquid Chromatography (UHPLC)-Time of Flight-MS was employed to examine endogenous analytes for inclusion in subsequent statistical analysis procedures used to analyse metabolic differences among the groups of samples. Metabolite extraction was done by fractionating the samples into pools of species with similar physicochemical properties, using appropriate combinations of organic solvents. Then, two separate UHPLC-MS platforms optimized for a wide coverage of the cardiac tissue lipidome were employed [27], allowing the optimal profiling of (1) Fatty acyls, bile acids, steroids and lysoglycerophospholipids; (2) Glycerolipids, glycerophospholipids, sterol lipids and sphingolipids. Lipid nomenclature and classification follow the LIPID MAPS convention, www.lipidmaps.org. Metabolite extraction procedures, chromatographic separation conditions, and mass spectrometric detection conditions are detailed in Barr et al. [27].

2.8. Cell culture and treatments

The HL-1 is a cardiomyocyte cell line derived from the AT-1 mouse atrial cardiomyocyte lineage, established and previously described by Claycomb et al. [28]. Before culture cells, dishes were coated with 0.5 % bovine fibronectin (Sigma) in 0.02 % gelatin overnight at 37 °C. HL-1 cells were cultured in Claycomb's specific media (SIGMA #51800C) supplemented with 10 % fetal bovine serum (GIBCO, Thermo Fisher Scientific, USA, Cat #10270106), 2 mM L-glutamine (GIBCO, Thermo Fisher Scientific, USA, Cat #25030–081), Penicillin-Streptomycin (5000 U/ml) (GIBCO, Thermo Fisher Scientific, USA, Cat #15070063) and grown at 37 °C in a 5 % CO2 incubator. After culturing for 24 h (30–50 % confluency) in supplemented Claycomb's medium, cells were washed with serum-free Claycomb's medium and cultured in Dulbecco's Modified Essential Media (DMEM) medium prior to treatment with experimental conditions.

To evaluate the gene expression of fibrotic and lipid metabolism markers, after 6-h starvation, cells were incubated for 24-h with sodium palmitate (PAL) (100 μM) (Sigma-Aldrich, USA Cat #P9767). PAL powder was dissolved in EtOH, diluted in a medium with 1 % fatty acid-free BSA (Sigma-Aldrich, USA Cat #A4503) and wormed to 57 °C to prepare a stock solution (50 mM). 1 h before the challenge, cells were pretreated with OEA (3 μM) or a PPAR-α agonist, GW7647 (1 μM) (Tocris Bioscience, UK, cat #1677). The cells were stimulated 30 min before the treatments with a PPAR-α antagonist, GW6471 (2 μM) (Tocris Bioscience, UK, cat #4618) and TRPV1 antagonist, capsazepine (5 μM)

(Sigma-Aldrich, USA Cat #C191). Total RNA was isolated and extracted as reported below.

2.9. Western blotting

Heart was homogenized in lysis buffer (20 mM Tris–HCl, pH 7,5, 10 mM NaF, 150 mM NaCl, 1 % Nonidet P-40, 1 mM phenyl-methylsulphonyl fluoride, 1 mM Na3VO4, leupeptin 10 μg/ml, and trypsin inhibitor 10 μg/ml) with a homogenizer (Ultra-Turrax T8; IKA Labortechnik, DEU). Total protein lysates were obtained as supernatant by centrifugation at $14,000 \times g$ for 15 min at 4 °C. Protein concentrations were estimated by the Bio-Rad protein assay using free bovine serum albumin (BSA) as standard. An equal amount of protein (30 μg) was subjected to SDS-PAGE and electro-transferred onto a nitrocellulose membrane using a Bio-Rad Transblot (Bio-Rad, Milan, Italy). The following parameters were set: 10 min of blotting time, 1.3 mA (approximately 25 V). The membrane was then blocked with $1 \times$ phosphate buffer solution (PBS) and 5 % non-fat dried milk for 45 min at RT and was incubated rabbit polyclonal antibodies against Phospho-AMPKα (Thr172) (1:1000; Cat #2531), AMPKα (1:1000; Cat #2532), Phospho-AKT (Thr308) (1:1000; Cat #4056), Phospho-AKT (Ser473) (1:1000; Cat #9271), AKT (1:1000; Cat #9272), Phospho-AS160 (Ser588) (1:1000; Cat #8730); AS160 (1:1000; Cat #2670); LC3B (1:1000; Cat #2775) and SQSTM1/p62 (1:1000; Cat #5114) from Cell Signaling Technology, Inc. (USA) and GLUT4 (#AF5386) from Affinity Biosciences (USA). Glyceraldehyde-3-phosphate dehydrogenase (GAPDH) (1:8000; Sigma-Aldrich USA; Cat #G9545) was used to normalize and ensure equal sample loading. We employed mouse anti-rabbit IgG-HRP (1:1000; sc-2357) from Santa Cruz Biotechnology, Inc. (USA) as a secondary antibody. Visualization of protein band intensities was determined by chemiluminescence using ChemiDoc MP Imaging System (Bio-Rad Laboratories, Inc., USA).

2.10. Real-time PCR analysis

Total RNA was isolated from the heart or cells using TRIzol Reagent (Bio-Rad Laboratories, USA) through the NucleoSpin kit (Macherey-Nagel cod.740955.50), according to the manufacturer's instructions. In terms of quality and quantity, total RNA was measured using a Nano-Drop One spectrophotometer (Thermo Fisher Scientific, USA). RNA samples with a 260/280 ratio between 2.0 and 2.2 were considered qualified. cDNA was obtained using a High-Capacity cDNA Reverse Transcription Kit (cod. 4374966, Thermo Fisher Scientific, USA) from 4 μg of total RNA. PCRs were performed on the Bio-Rad CFX96 Connect Real-time PCR System instrument and software (CFX Maestro Software). PCR conditions were 15 min at 95 °C followed by 40 cycles of two-step PCR denaturation at 94 °C for 15 s, annealing extension at 55 °C for 30 s and extension at 72 °C for 30 s. Each sample contained 500 ng of cDNA in $2 \times$ QuantiTect SYBR Green PCR Master Mix (cod. 204145, Qiagen, DEU) and primers pairs to amplify mouse interleukin (IL)-1β (*Il1b*), IL-6 (*Il6*), chemokine (C—C motif) ligand 2 also referred as monocyte chemoattractant protein (MCP)1 (*Ccl2*), transforming growth factor beta 1 (*Tgfb1*), fibrillin 1 (*Fbn1*), collagen type I alpha 1 chain (*Col1a1*), collagen type III alpha 1 chain (*Col3a1*), cluster of differentiation 36 (*Cd36*), peroxisome proliferator-activated receptor alpha (*Ppara*), fatty acid synthase (*Fasn*), adiponectin (*Adipoq*), meteorin-like protein (*Metrnl*), autophagy-related 3, 5 and 7 (*Apg3l*) (*Apg5l*) (*Apg7l*) (Qiagen, DEU) in a final volume of 50 μl. The relative amount of each studied mRNA was normalized to mouse *Rn18s* (Qiagen, DEU) as a housekeeping gene, and data were analyzed according to the $2^{-\Delta\Delta CT}$ method.

2.11. Data and statistical analysis

All experimental data are presented as the mean ± Standard Error of the Mean (SEM) of at least 5 individual measurements per group with *n* defined as independent animal individuals and subjected to one-way

variance analysis (ANOVA) for multiple comparisons followed by Bonferroni's post hoc test, using GraphPad Prism 8 (GraphPad Software Inc., USA).

Metabolomics data were pre-processed employing the TargetLynx application manager for MassLynx 4.1 (Waters Corp., US). Intra-batch (multiple internal standard response correction) and inter-batch (variable specific inter-batch single point external calibration using repeat extracts of a commercial serum sample) normalization followed the method described in Martínez-Arranz et al., [29]. All calculations for metabolomic data were carried out using the statistical software package R v.3.1.1 (R Development Core Team, 2011, AT; https://cran.r-pro ject.org/) and Python 3.7.9 (Python Software Foundation, NL). Differences among groups were considered significant at values of $P < 0.05$.

3. Results

3.1. OEA counteracts metabolic alterations induced by HFD in mice

The body weight of all mice was monitored during the whole treatment period. HFD-fed mice showed a significant increase in body weight gain compared to mice fed with a STD diet. OEA treatment gradually and significantly reduced body weight gain (Fig. 1A) starting from the 3rd week of treatment when compared to untreated HFD mice. AUC of body weight gain throughout the treatment period was also obtained (Fig. 1B). Consistently, obese mice showed a significant increase in the AUC of body weight gain during the experimental time of treatment, which was significantly decreased by OEA treatment. Daily energy intake (evaluated at the end of the 8th week of treatment) of OEA-treated mice was significantly lower than that of HFD mice (Fig. 1C). Regarding the analysis of body composition, the increased fat mass observed in HFD mice was significantly reduced in OEA-treated mice (Fig. 1D). To investigate the metabolic function and to assess glucose metabolism specifically, OGTT was performed. In the HFD group, blood glucose levels were significantly higher at each analyzed time point compared to those of STD mice, indicating an alteration of glucose disposal (Fig. 1E). Conversely, OEA treatment limited the alteration of glycemia during time, and the relative AUC, as shown in the upper panel. Accordingly, OEA significantly decreased fasting glycemic levels, which were incremented by HFD (Fig. 1F). OEA also significantly reduced heart weight, which was significantly increased in HFD mice (Fig. 1G). Moreover, serum cholesterol (Fig. 1H) and CK-MB (Fig. 1I) levels were significantly reduced in OEA-treated mice when compared to those on HFD.

3.2. OEA increased the phosphorylation of AMPK, AKT and AS160 in the cardiac tissue of obese mice

Taking into account that AMPK, AKT and AS160 are involved in glucose uptake and GLUT4 translocation at the cardiac level [30], and in order to decipher the modulatory effect of OEA on cardiac energetic metabolism, the phosphorylation of AMPK, AKT and AS160 was evaluated in the heart of mice from all groups. Notably, OEA significantly increased the phosphorylation of AMPK (Fig. 2A and B), AKT at the Ser473 and Thr308 sites (Fig. 2A, C and D), and AS160 (Fig. 2A and E) compared to HFD mice. Consistently, GLUT4 expression was increased by OEA treatment in cardiac tissues of HFD mice (Fig. 2A and F).

3.3. Effect of OEA on the lipidome of cardiac tissue from mice fed an HFD

OEA levels were increased in the cardiac tissue as the effect of the HFD ($p < 0.001$) and clearly increased in mice receiving the treatment with OEA (Fig. 3A). This metabolite is also an endogenous metabolite and, thus, can be detected in non-treated samples. This result demonstrates that our experiment has been performed correctly, and the OEA treatment has functioned efficiently. Additionally, OEA significantly increased the levels of the N-acyl ethanolamines (NAE) metabolic class

in the cardiac tissue of HFD mice (Fig. 3B).

Only seven metabolites out of 364 were significantly altered in the comparison HFD + OEA vs HFD, being an N-acyl ethanolamine, a monoglyceride, two lysophosphatidylethanolamines and three sphingomyelins (SM) (Supplementary Table 1). Remarkably, OEA treatment regulates (or partially regulates) the changes induced by the HFD in the levels of the sphingomyelins for SM (d18:1/23:0) (Fig. 3C), SM (43:1) (Fig. 3D), and SM (38:0) (Fig. 3E). This effect on sphingomyelin levels is interesting, as these sphingolipids have been previously related to coronary heart disease and cardiovascular diseases [31]. Considering the relevance of different specific lipids at cardiac metabolic level, we have also analyzed the possible changes in 84 species of triacylglycerols (TG), total TG, 10 diacylglycerols (DG), total DG, 13 ceramides (Cer), total Cer), and cholesterol. However, we were not able to find significant changes in the cardiac levels of these metabolites in the comparison of HFD + OEA vs. HFD. Moreover, we have performed the lipidomic comparison of HFD vs. STD and HFD + OEA vs. STD and we have found that the DG species DG(38:5) ($\log_2$ (fold change) = 0.490, p-value = 0.010) and TG(52:4) ($\log_2$ (fold change) = 1.526, p-value = 0.028) were significantly increased while the Cer species Cer(d18:1/23:0) ($\log_2$ (fold change) = −0.289, p-value = 0.015) and Cer(d18:1/25:0) ($\log_2$ (fold change) = −0.289, p-value = 0.038) were significantly decreased in cardiac tissue by HFD when compared to STD. These changes were not observed when mice fed with HFD were treated with OEA and compared to STD animals.

3.4. OEA treatment affects lipid metabolism and adipokine expression in the heart of obese mice

To define the effect of OEA on cardiac lipid homeostasis, we determined the mRNA expression of the fatty acid translocase CD36 and the fatty acid synthase (FASN), known to regulate lipid uptake and synthesis in cardiomyocytes, respectively [32,33]. The overexpression of both genes in the ventricles of HFD-fed mice was blunted by OEA treatment, indicating a reduction of cardiac lipid accumulation (Fig. 4A, B). We have also evaluated the effect of OEA on Ppara gene expression levels, involved in lipid metabolism in the heart [34,35]. OEA treatment significantly increased the mRNA levels of this gene, which was unchanged in the hearts of HFD mice compared to STD (Fig. 4C). Moreover, OEA normalized the increased mRNA levels of adiponectin (Fig. 4D) and meteorin-like (Fig. 4E) in the cardiac tissues of HFD mice, indicating a marked activity in regulating cardiovascular function.

3.5. OEA decreases inflammation and fibrosis in the cardiac tissue of obese mice

OEA showed a marked anti-inflammatory effect in the heart ventricle of HFD mice by significantly counteracting the increased mRNA levels of the pro-inflammatory mediators IL-1β, TNF-α, IL-6, and MCP-1 (Ccl2) in HFD mice (Fig. 5A). Moreover, OEA treatment significantly reduced the cardiac gene expression levels of the pro-fibrotic factors TGF-β1, fibrillin 1 (Fbn1), collagen type I (Col1a1) and collagen type III (Col3a1), which were significantly increased in HFD mice (Fig. 5B).

3.6. OEA treatment induces autophagy in the heart of HFD mice

The effect of OEA on cardiac autophagy was investigated by evaluating protein levels of the autophagic markers LC3B and p62 in mice. OEA treatment significantly increased the ratio between isoform II and I of LC3B (Fig. 6A) and reduced the protein expression levels of p62 (Fig. 6B) in the heart of HFD mice, indicating a stimulation of the autophagic process at the cardiac level. Autophagy-related genes, specifically Apg3l, Apg5l, and Apg7l, which are known to mediate autophagy, were also analyzed by Real-Time PCR (Fig. 6C-E). Notably, their cardiac transcription was upregulated in OEA-treated mice, confirming an enhanced autophagy process in cardiac tissues.
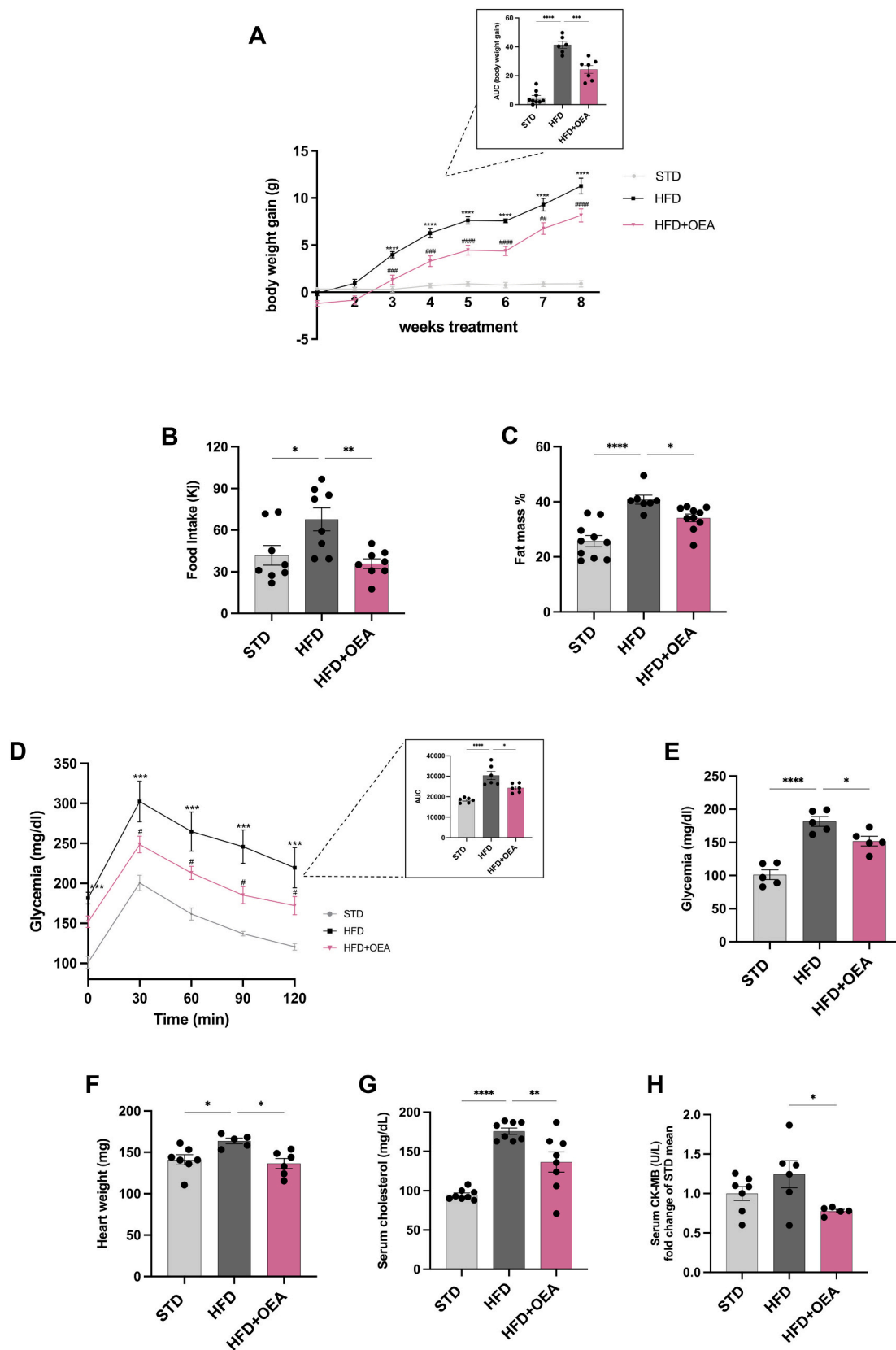
Fig. 1. OEA treatment regains metabolic parameters altered by HFD. Body weight gain (A) was measured weekly during the treatment period. Similar results were obtained by evaluating the respective AUC (B). Furthermore, food intake, expressed in Kilojoule (Kj) (C) and fat mass (D) were evaluated. Moreover, before sacrifice, OGTT was performed in all groups of animals (E). Glucose levels in fasted mice are also shown (F). Heart weight (G), serum cholesterol (H) and serum CK-MB (I) were examined. Results are shown as mean ± S.E.M (*vs STD; # vs HFD for panels A and E). (*/#$P < 0,05$, **/##$P < 0,01$, ***/###$P < 0.001$, and ****/####$P < 0,0001$).
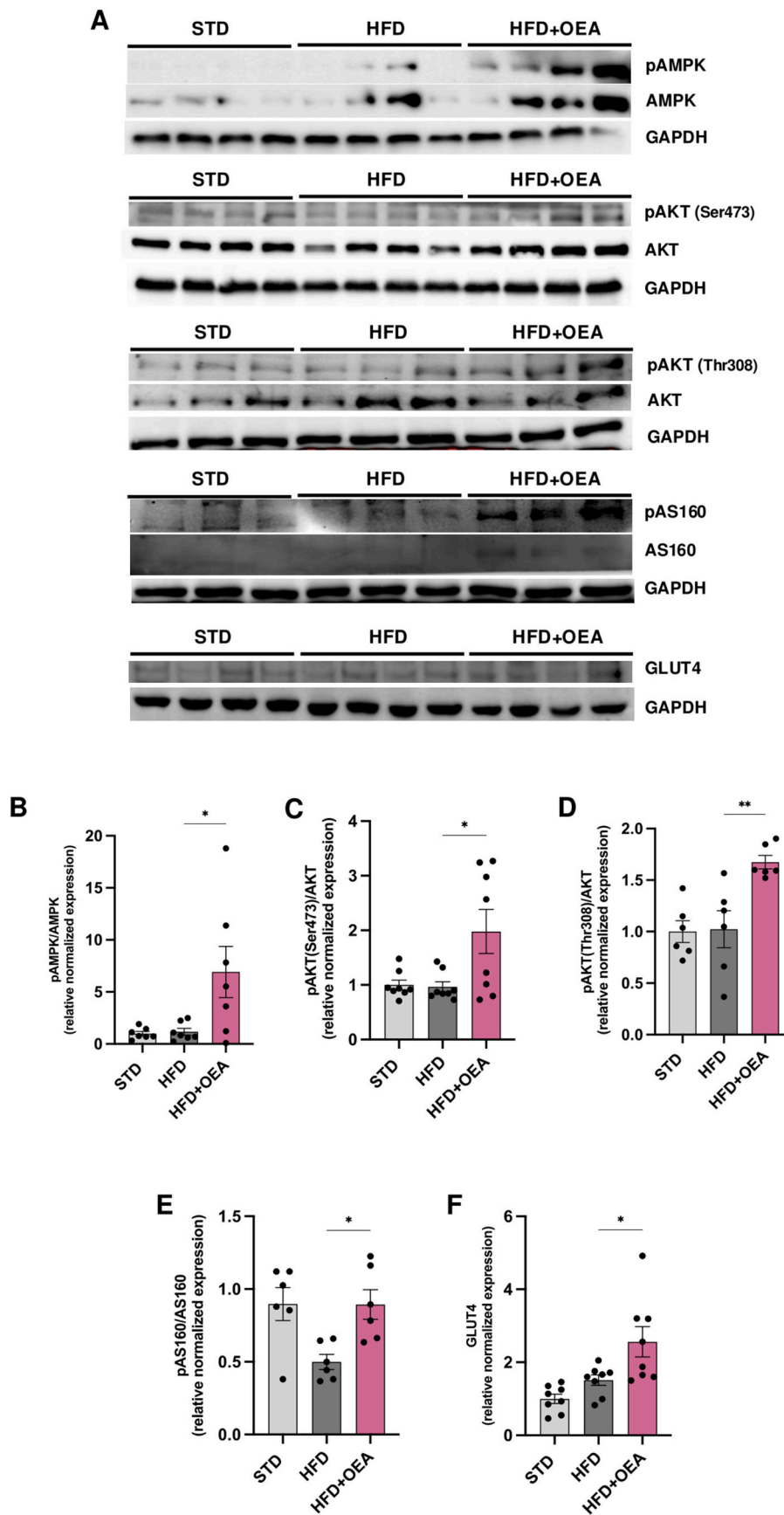
Fig. 2. OEA induces the activation of AMPK-AKT-AS160 pathways. Representative photographs of Western blot (A) and statistical analysis data of the ratio of phosphorylated AMPK (B), AKT serine 473 (C), AKT threonine 308 (D), AS160 (E) on the total protein and GLUT-4 (F) in cardiac ventricles were shown. Results are displayed as mean ± S.E.M (*P < 0,05 and **P < 0,01).
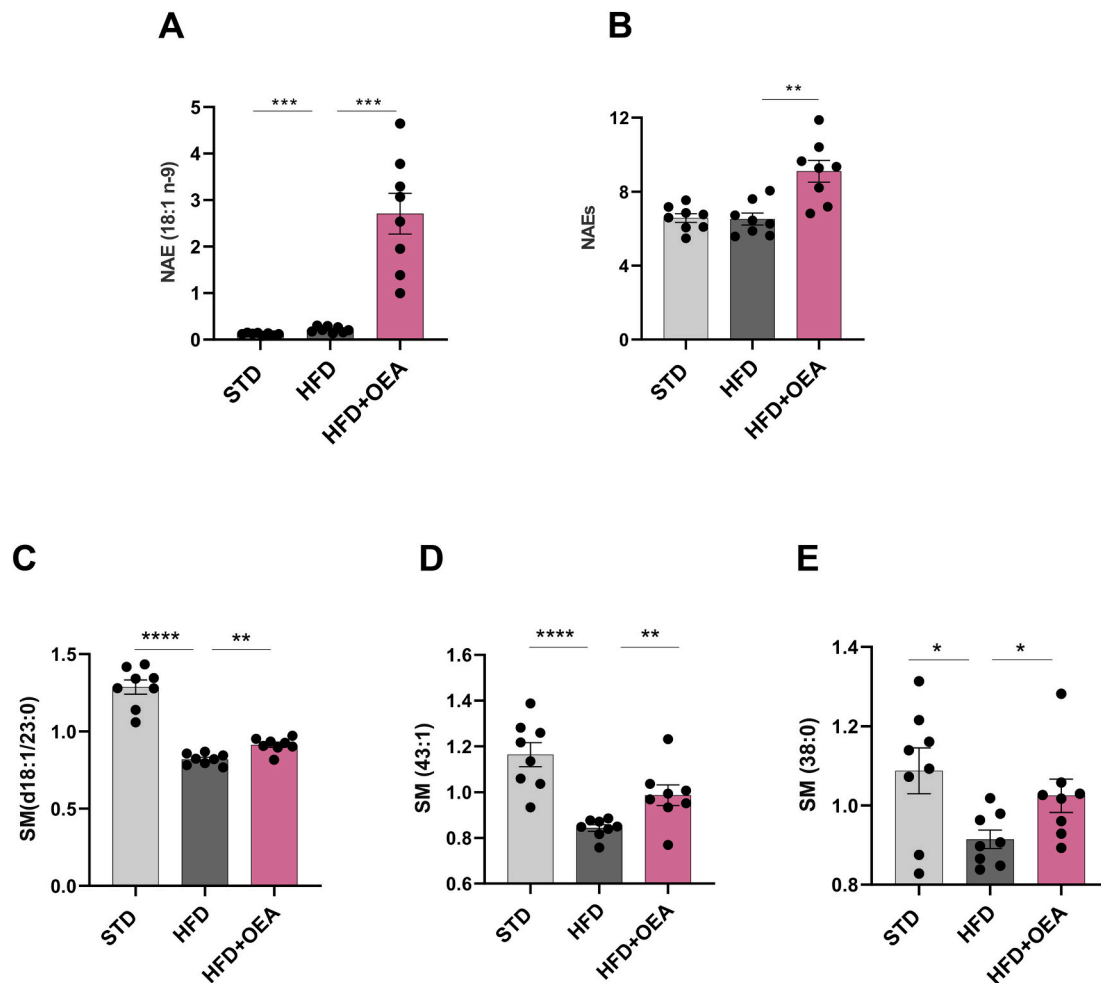
Fig. 3. Metabolite classes significantly altered in the unpaired comparisons HFD vs STD and HFD + OEA vs STD, and individual metabolites significantly altered in the comparison HFD + OEA vs HFD. OEA treatment modified in cardiac tissue the levels of NAE (18:1 n-9) (A), the NAE (B) metabolic class, the SM (d18:1/23:0) (C), SM (43:1) (D), and SM (38:0) (E) when compared to HFD mice. Data are shown as mean ± S.E.M ($*p < 0.05$, $**p < 0.01$, $***p < 0.001$ and $****p < 0.0001$). Unpaired Wilcoxon test. NAE: N-acyl ethanolamines, SM: Sphingomyelin.

### 3.7. Direct activity of OEA in palmitate-challenged cardiomyocytes: PPAR-α involvement

To evaluate the direct activity on cardiac cells and provide mechanistic insight by OEA, we set up an in vitro model using HL-1 cardiomyocytes insulted by palmitate, as metabolic challenge. Cell treatment with OEA reduced palmitate-induced transcription of the *Ccl2* and *Tnf* gene (Fig. 7A and B), as well as TGF-β1 and fibrillin 1 (Fig. 7C and D). Notably, GW6471-mediated antagonism of PPAR-α induced a trend of reversal of OEA anti-inflammatory effect (Fig. 7A and B) and significantly blunted OEA effect on *Tgfb1* and *Fbn1* mRNAs (Fig. 7C and D). Furthermore, GW7647, a synthetic PPAR-α agonist, showed a OEA-like effect on all analyzed markers (Fig. 7A-D).

4. Discussion

OEA effect was evaluated in an HFD-induced obesity model to assess its beneficial potential in mice affected by dysfunctional metabolism. Following long-term HFD feeding, mice show metabolic derangement recapitulating those observed in metabolic syndrome in humans, e.g. obesity, insulin resistance, and altered serum glycemic and lipid profile [36,37]. Weight gain is a hallmark of the development of metabolic syndrome and is shown in all the studies that display metabolic syndrome and type 2 diabetes by keeping animals on HFD [38]. In our experimental conditions, OEA significantly counteracted the increase in

energy intake, inducing a mild decrease in weight gain from the third week of the treatment on, and in fat mass accumulation in HFD mice. Indeed, more profound weight gain and fat lowering effects were shown with higher doses of OEA ranging from 5 to 100 mg/kg in mice (Laleh et al., 2019). In line, OEA ameliorates serum fasting glucose and cholesterol levels, and improves glucose disposal from the systemic circulation, evaluated by oral glucose tolerance test. Notably, the heart weight and the level of serum CK-MB, a marker of myocardial damage, were decreased in OEA-treated obese mice compared to HFD mice, suggesting OEA cardioprotective effect. Obesity is a powerful promoter and predisposing factor for heart hypertrophy and failure [39] since it causes chronic structural changes sustained by several detrimental mechanisms, including disorders in cardiac metabolism, inflammation, autophagy, and fibrosis [40].

In cardiac muscle, AMPK, a cellular energy sensor, has a specific role in the regulation of cardiomyocyte metabolism, modulating myocardial substrate utilization depending on the availability of energy substrates, hormonal conditions, and workload. Indeed, an increase in AMPK activity in cardiomyocytes results in an increased rate of glucose uptake and β-oxidation of FA [41–44]. Here, the increased AMPK activation by OEA treatment was paralleled by AKT phosphorylation at the residues Thr308 and Ser473, indicating an increased insulin sensitivity in the cardiac tissue of HFD mice. Indeed, both pathways, triggered by OEA treatment, converge in AS160 phosphorylation and activation, which in turn induce the translocation of GLUT4 to the membrane, improving
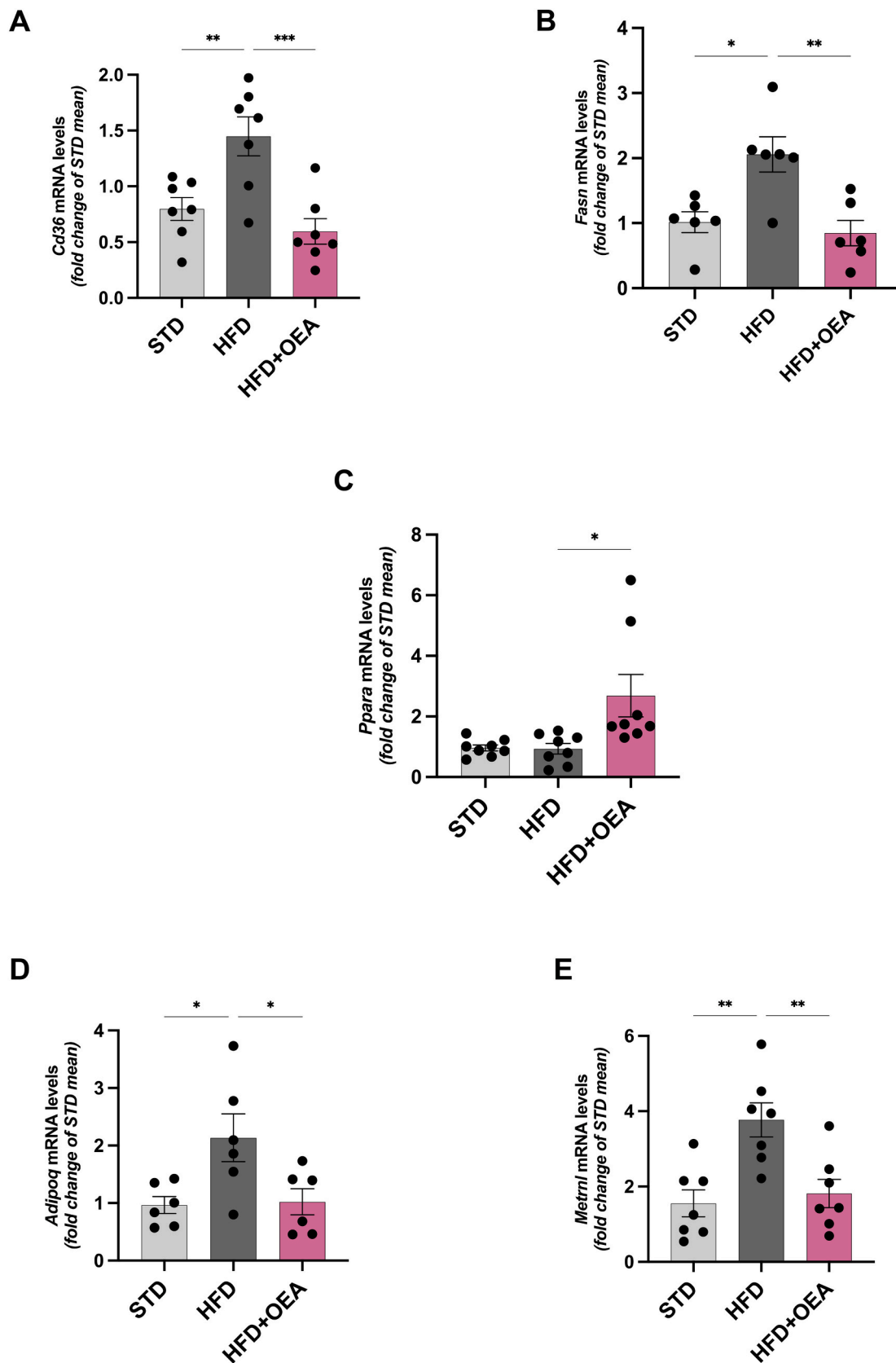
Fig. 4. OEA effect on the expression of cardiac metabolic mediators of mice on HFD. mRNA expression of the fatty acid transporter CD36 (A), fatty acid synthase (*Fasn*) (B), the peroxisome proliferator activating receptor-α (*Ppara*) (C), and the cardiac adipokines adiponectin (*Adipoq*) (D) and meteorin-like protein (*Metrnl*) (E) was detected in the cardiac tissues. Results are shown as mean ± S.E.M (*P < 0,05 **P < 0,01 and ***p < 0.001).
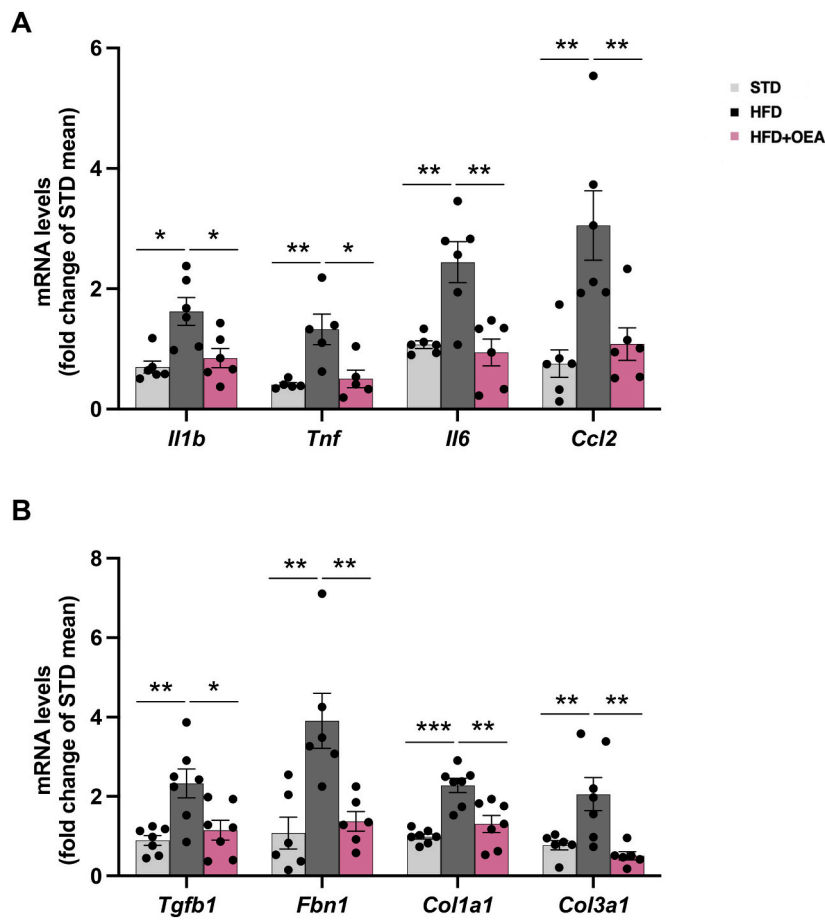
Fig. 5. OEA reduced cardiac proinflammatory and profibrotic mediators in obese mice. Gene expression of cytokines *Il1b*, *Tnf*, *Il6*, and chemokine *Ccl2* (A) associated with fibrotic parameters, such as *Tgfb1*, *Fbn1*, *Col1a1*, and *Col3a1* (B), was evaluated in ventricle tissues of all groups. Results are shown as mean ± S.E.M (*P < 0,05, **P < 0,01 and ***P < 0,001).

glucose uptake [45–47].

The detrimental increase in fatty acids and dysregulated adipokine secretion induced by HFD determines the maladaptive mechanisms in the heart that cannot counteract the metabolic alterations [48]. In cardiomyocytes, fatty acid synthesis is regulated by FASN, while their incoming flux is mainly regulated by the fatty acid translocase CD36 [49]. Here, in HFD mice, the increased transcription of both genes is suggestive of an excessive lipid accumulation along with the formation of lipotoxic species that can result in myocardial contractile dysfunction and promote insulin resistance. In cardiomyocytes, fatty acid synthesis is regulated by FASN, while their incoming flux is mainly regulated by the fatty acid translocase CD36 [52]. In accordance with our results, other authors have previously observed that cardiac FASN was significantly upregulated both in in vitro cultured cardiomyocytes treated with palmitic acid and in cardiac tissue from animal models of obesity induced by high fat diet [50,51]. Likewise, it is known that cardiac levels of CD36 are increased after high fat diet [52]. In this work, the increased expression of FASN and CD36 was instead countered by OEA in HFD mice, indicating a re-established cardiac fatty acid synthesis and flux homeostasis.

This increased expression of FASN and CD36 was instead countered by OEA in HFD mice, indicating a re-established cardiac fatty acid synthesis and flux homeostasis. Consistently, adiponectin and meteorin-like (Metrnl) transcription at the cardiac level was normalized by OEA treatment. Indeed, cardiomyocyte-derived adiponectin has a cardioprotective role through an autocrine/paracrine mechanism, directly impacting cardiac metabolism and preventing cardiovascular dysfunction [53,54]. As adiponectin, Metrnl, a newly discovered

cardioprotective factor, exhibits insulin-sensitizing and anti-inflammatory properties [54]. The induction of both adipokines at the cardiac level in HFD mice could represent a compensatory protective mechanism to limit myocardial dysfunction, which diminishes once metabolic homeostasis is achieved following OEA treatment. A metabolomic study of cardiac tissue samples taken from mice fed a control diet, an HFD, and mice fed HFD and treated with OEA was performed using ultra-high performance liquid chromatography-mass spectrometry. OEA was shown to cause relevant changes in the amounts of several classes of lipids found at cardiac level in HFD-fed mice. Our results reveal that OEA is able to induce a specific cardiac bioactive lipid profile. Although few changes were found in the heart' lipidome of HFD-fed mice as the effect of the OEA treatment, it can be highlighted the treatment seemed to attenuate the effects on the levels of several lipids. The most notable effect was observed in sphingomyelins. It is remarkable that OEA treatment reverses (or partially regulates) the changes induced by HFD in the levels of several sphingomyelins. This effect in sphingomyelin levels is noteworthy, as these sphingolipids are a lipid class with both signaling and structural properties that have been proposed as natural antioxidants [55] and have also been involved in inflammatory and immune responses, vascular homeostasis, insulin signaling, and diabetes [56,57].

HFD also leads to increased production of inflammatory cytokines IL-1, IL-6, and MCP-1, which play a crucial role in inflammatory cell recruitment and infiltration, compromising normal cardiomyocyte function and leading to myocardial fibrosis [58,59]. We showed that OEA exhibits a marked anti-inflammatory effect by reducing the transcription in the ventricle of such pro-inflammatory mediators involved
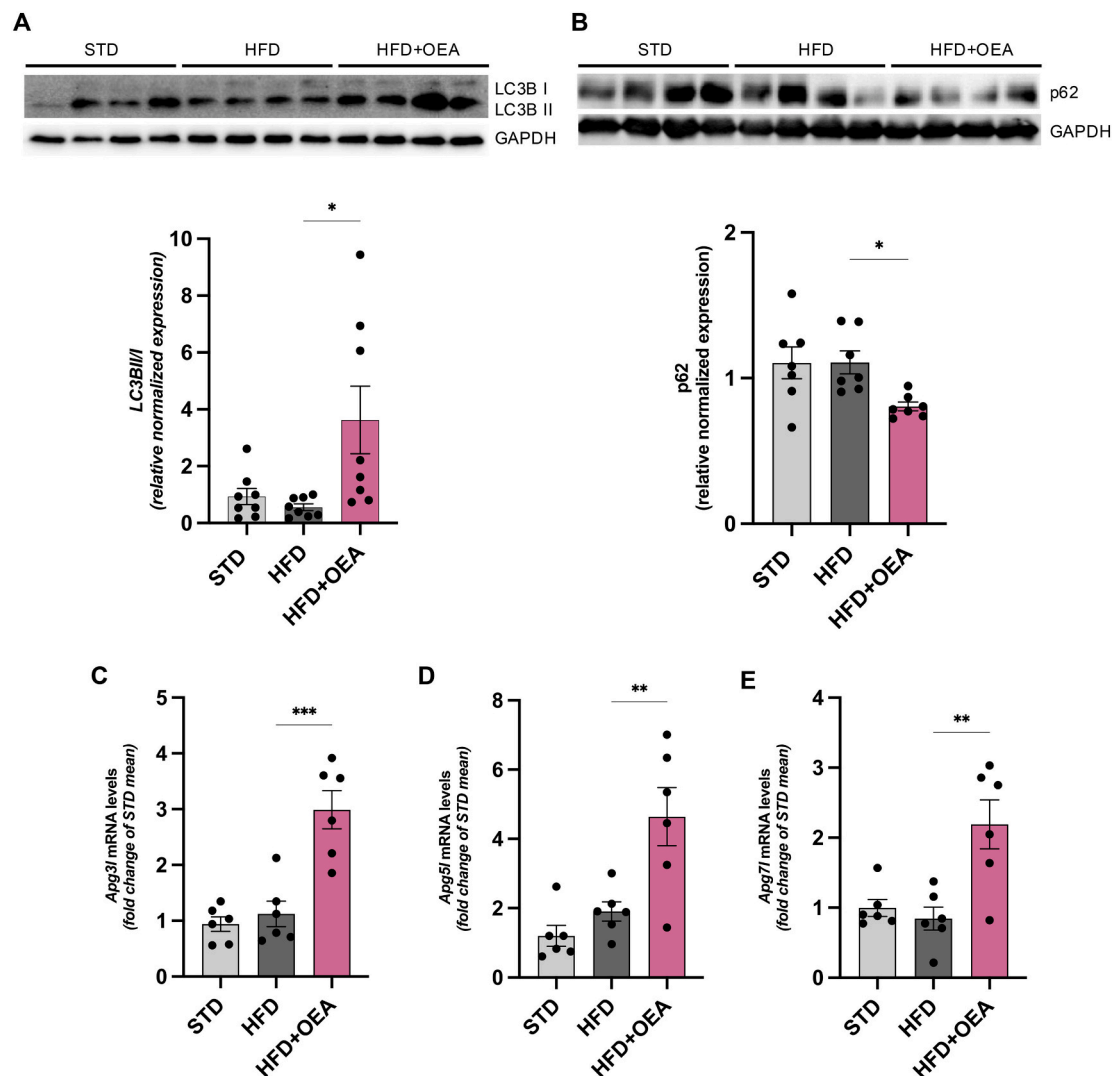
Fig. 6. OEA regulates cardiac autophagy in HFD mice. OEA treatment modulates the protein expression of the autophagosome membrane markers of autophagy LC3II/I (A), increasing their ratio and decreasing the cardiac level of p62/SQSTM1 (B). Moreover, OEA increased the mRNA expression of 3 different autophagy-related factors such as *Agp3l* (C), *Agp5l* (D) and *Agp7l* (E). Results are shown as mean ± S.E.M (*P < 0,05, **P < 0,01 and ***P < 0,001).

in the progression of heart damage and cardiac remodeling [60]. Accordingly, OEA was able to limit cardiac fibrosis, reducing the expression of all the profibrotic markers that were markedly increased in the heart from HFD mice, i.e. TGF-β1, fibrillin 1, collagen I and III, that participate in forming the extracellular matrix [61].

During the pathogenesis of obesity-related cardiovascular disease, the dysregulation of lipid and glucose metabolism has also been shown to affect the autophagic response in the heart, accelerating cardiac remodeling. The basal autophagy process constitutes an essential mechanism in cardiomyocyte function by renewing and recycling cytoplasmic components, organelles or protein aggregates whose accumulation can be cytotoxic [62]. We showed that OEA stimulates the autophagic process, modulating the processing of LC3 protein and the expression of p62 protein. LC3 protein, initially synthesized as an unprocessed proLC3 form, undergoes a proteolytic modification to obtain the soluble cytosolic form LC3I [63]. During the induction of the autophagic process, LC3I undergoes covalent lipidation, producing the conjugated form LC3II, located in the autophagic membranes associated with the autophagosome; this way, evaluating LC3II as an autophagic marker provides an approximate interpretation of phagosome numbers, although it does not provide information on autophagic flux [64].

Moreover, p62 protein (also called sequestosoma 1, SQSTM1) degradation by the autophagosome through its interaction with LC3 could be an additional event indicative of an increased cellular autophagy flux [65]. The increased LC3II/LC3I ratio, along with the decrease of p62 expression by OEA treatment, was indicative of an increase in the autophagic process, a finding strengthened by the increase in the autophagic markers Apg3, Apg5 and Apg7 [66].

Our data show a significant, albeit slight, impact of OEA on the metabolic profile of obese mice, limiting body weight gain, and reducing fat mass and glucose intolerance, which potentially contributes to the cardiac beneficial effect of OEA. However, here, we also observed a possible tissue-specific cardioprotective activity by OEA since we found an increase of NAEs, specifically of OEA, as well as of PPAR-α expression in the heart of OEA-treated HFD mice. Consistently, in experiments on HL-1 cells, we have demonstrated OEA's capability in reducing the expression of pro-inflammatory and pro-fibrotic genes, mimicking in vitro the cardiac metabolic alterations through palmitate challenge. OEA protective effect has also been demonstrated against doxorubicin-induced cardiotoxicity in mice [21], a non-metabolic model of cardiac damage. These authors showed a direct TRPV1-mediated mechanism underlying the OEA effect, free of any metabolic-dependent
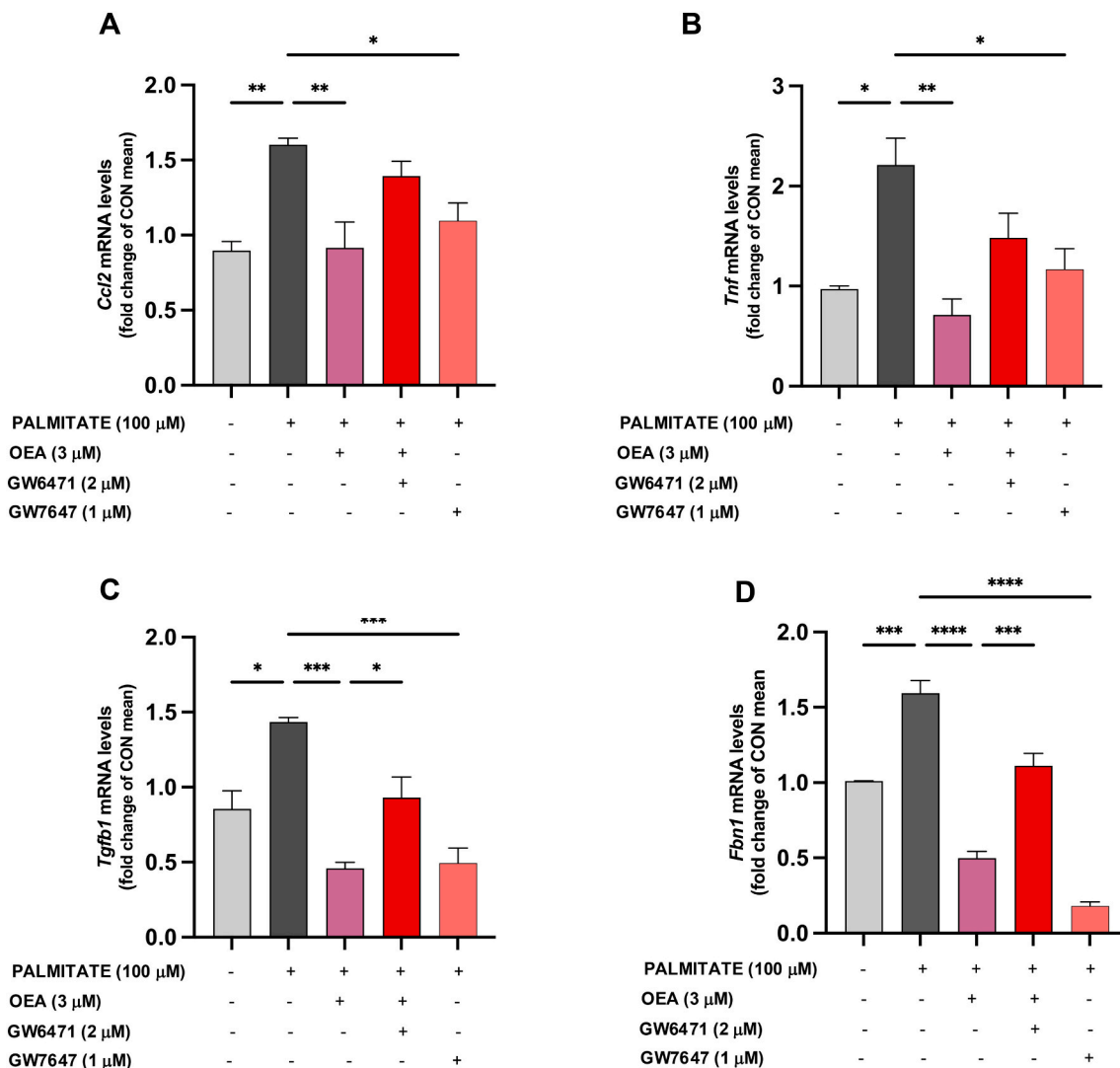
Fig. 7. OEA exerts similar activities as the synthetic PPAR-α agonist in limiting inflammation and fibrosis following palmitate challenge in HL-1 cells. Gene expression of *Ccl2* (A), *Tnf* (B), *Tgfb1* (C) and *Fbn1* (D) was evaluated in HL-1 cells challenged with palmitate, pretreated or not with the PPARα antagonist GW6471, and stimulated with OEA or the PPARα synthetic agonist, GW7647. Results are shown as mean ± S.E.M ($*P < 0,05$, $**P < 0.01$, $***P < 0,001$ and $****P < 0,0001$).

contribution. Here, in in vitro experiments, we showed OEA-like protective activities by treating HL-1 cells with GW7647, a synthetic PPAR-α agonist, without any intrinsic activity on TRPV1. The involvement of PPAR-α activation in OEA effects was also strengthened by the reduced anti-inflammatory and anti-fibrotic activity of OEA in the presence of the selective PPAR-α antagonist GW6471.

However, with this premise, the partial reversal of OEA effect by the PPAR-α antagonist does not exclude alternative protective receptors and pathways other than those under PPAR-α control.

PPAR-α plays a role in maintaining the homeostasis of myocardial energy metabolism [67]. It regulates critical genes implicated in the β-oxidation cycle, as well as those regulating the incoming of fatty acids into mitochondria [68]. Notably, PPAR-α deficiency in the myocardium has been associated to progressive cardiac fibrosis, pathological myofibrils, and abnormal mitochondria [34,69]. Moreover, literature data have indicated a role for PPAR-α binding NAEs, in particular OEA and palmitoylethanolamide (PEA), in several cardiometabolic diseases, such as atherosclerosis [70,71]; PEA cardioprotective effect was also demonstrated in ischemia/reperfusion induced myocardial injury in vivo [72] and in vitro [73]. Accordingly, our studies on spontaneously hypertensive rats have demonstrated that chronic treatment with PEA

reduced hypertension, by improving endothelium derived hyperpolarizing factors -mediated vasodilation, and renin-angiotensin system in the vasculature [74]. Currently, pharmacological targeting of PPAR-α has been demonstrated to be a relevant strategy for patients with diabetes and cardiometabolic diseases [75,76]. A better understanding of the cellular effects of PPAR-α activation in the cardiovascular system, in addition to its lipid-lowering influence, shall further promote the development and clinical application of new PPAR-α agonists.

There are a few limitations of this study that need to be addressed. First, the inability of this animal model of obesity lasting many weeks to provide mechanistic insight into the involvement and the possible contribution of the key receptors among those underlined to OEA effect. Therefore, a focus on OEA mechanisms was achieved through an in vitro approach on cardiomyocytes. Second, OEA rescuing effect on the cardiac functional status, known to be altered following HFD feeding, was not evaluated. This issue would enable to correlate molecular and biochemical evaluations (e.g. inflammatory and fibrotic parameters, CK-MB) with the extent of heart functional improvement.

Taken together, our results indicate OEA as a potential therapeutic to restrain cardiac complications associated with metabolic disorders, being able to counteract both pathological mechanisms external to the

heart related to overall metabolic homeostasis and intrinsic cardiac molecular mechanisms, including lipotoxicity, tissue inflammation and fibrosis.

Supplementary materials to this article can be found online at https://doi.org/10.1016/j.lfs.2024.123226.

CRediT authorship contribution statement

Federica Comella: Investigation. **Alana Aragón-Herrera:** Investigation. **Claudio Pirozzi:** Investigation, Data curation. **Sandra Feijóo-Bandín:** Investigation. **Adriano Lama:** Investigation. **Nicola Opallo:** Investigation. **Stefania Melini:** Investigation. **Filomena Del Piano:** Investigation. **Oreste Gualillo:** Validation, Supervision. **Rosaria Meli:** Validation, Supervision, Data curation. **Giuseppina Mattace Raso:** Writing – review & editing, Writing – original draft, Supervision, Data curation, Conceptualization. **Francisca Lago:** Writing – review & editing, Writing – original draft, Validation, Supervision, Data curation, Conceptualization.

Declaration of competing interest

The authors declare the following financial interests/personal relationships which may be considered as potential competing interests.

References

[1] M.E. Piché, A. Tchernof, J.P. Després, Obesity Phenotypes, Diabetes, and Cardiovascular Diseases, Circ. Res. 126 (11) (2020 May 22) 1477–1500, https://doi.org/10.1161/CIRCRESAHA.120.316101. Epub 2020 May 21. Erratum in: Circ Res. 2020 Jul 17;127(3):e107. doi: https://doi.org/10.1161/RES.0000000000000421, 32437302.

[2] J. Ren, N.N. Wu, S. Wang, J.R. Sowers, Y. Zhang, Obesity cardiomyopathy: evidence, mechanisms, and therapeutic implications, Physiol. Rev. 101 (4) (2021 Oct 1) 1745–1807, https://doi.org/10.1152/physrev.00030.2020 (Epub 2021 May 5. PMID: 33949876; PMCID: PMC8422427).

[3] L. Pulakat, V.G. DeMarco, S. Ardhanari, A. Chockalingam, R. Gul, A. Whaley-Connell, J.R. Sowers, Adaptive mechanisms to compensate for overnutrition-induced cardiovascular abnormalities, Am. J. Physiol. Regul. Integr. Comp. Physiol. 301 (4) (2011 Oct) R885–R895, https://doi.org/10.1152/ajpregu.00316.2011 (Epub 2011 Aug 3. PMID: 21813874; PMCID: PMC3289980).

[4] G.D. Lopaschuk, Q.G. Karwi, R. Tian, A.R. Wende, E.D. Abel, Cardiac Energy Metabolism in Heart Failure, Circ. Res. 128 (10) (2021 May 13) 1487–1513, https://doi.org/10.1161/CIRCRESAHA.121.318241 (Epub 2021 May 13. PMID: 33983836; PMCID: PMC8136750).

[5] R. Romero-Becera, A.M. Santamans, A.C. Arcones, G. Sabio, From Beats to Metabolism: the Heart at the Core of Interorgan Metabolic Cross Talk, Physiology (Bethesda) 39 (2) (2024 Mar 1) 98–125, https://doi.org/10.1152/physiol.00018.2023 (Epub 2023 Dec 5. PMID: 38051123).

[6] Q.G. Karwi, G.M. Uddin, K.L. Ho, G.D. Lopaschuk, Loss of Metabolic Flexibility in the Failing Heart, Front Cardiovasc Med. 5 (2018 Jun 6) 68, https://doi.org/10.3389/fcvm.2018.00068 (PMID: 29928647; PMCID: PMC5997788).

[7] Q. Sun, B. Güven, C.S. Wagg, A. Almeida de Oliveira, H. Silver, L. Zhang, B. Chen, K. Wei, E.B. Ketema, Q.G. Karwi, K.L. Persad, J. Vu, F. Wang, J.R.B. Dyck, G.Y. Oudit, G.D. Lopaschuk, Mitochondrial fatty acid oxidation is the major source of cardiac adenosine triphosphate production in heart failure with preserved ejection fraction, Cardiovasc. Res. 120 (4) (2024 Mar 30) 360–371, https://doi.org/10.1093/cvr/cvae006 (PMID: 38193548).

[8] C.M. Depner, M. Torres-Gonzalez, S. Tripathy, G. Milne, D.B. Jump, Menhaden oil decreases high-fat diet-induced markers of hepatic damage, steatosis, inflammation, and fibrosis in obese Ldlr−/− mice, J. Nutr. 142 (8) (2012 Aug) 1495–1503, https://doi.org/10.3945/jn.112.158865 (Epub 2012 Jun 27. PMID: 22739374; PMCID: PMC3397337).

[9] Y. Hua, Y. Zhang, J. Dolence, G.P. Shi, J. Ren, S. Nair, Cathepsin K knockout mitigates high-fat diet-induced cardiac hypertrophy and contractile dysfunction, Diabetes 62 (2) (2013 Feb) 498–509, https://doi.org/10.2337/db12-0350 (Epub 2012 Oct 15. PMID: 23069627; PMCID: PMC3554365).

[10] Z. Pan, X. Sun, H. Shan, N. Wang, J. Wang, J. Ren, S. Feng, L. Xie, C. Lu, Y. Yuan, Y. Zhang, Y. Wang, Y. Lu, B. Yang, MicroRNA-101 inhibited postinfarct cardiac fibrosis and improved left ventricular compliance via the FBJ osteosarcoma oncogene/transforming growth factor-β1 pathway, Circulation 126 (7) (2012 Aug 14) 840–850, https://doi.org/10.1161/CIRCULATIONAHA.112.094524 (Epub 2012 Jul 18. PMID: 22811578).

[11] P. Ayala, J. Montenegro, R. Vivar, A. Letelier, P.A. Urroz, M. Copaja, D. Pivet, C. Humeres, R. Troncoso, J.M. Vicencio, J. Lavandero, G. Díaz-Araya, Attenuation of endoplasmic reticulum stress using the chemical chaperone 4-phenylbutyric acid prevents cardiac fibrosis induced by isoproterenol, Exp. Mol. Pathol. 92 (1) (2012 Feb) 97–104, https://doi.org/10.1016/j.yexmp.2011.10.012. Epub 2011 Nov 10. Erratum in: Exp Mol Pathol. 2021 Aug;121:104669. doi: https://doi.org/10.1016/j.yexmp.2021.104669, 22101259.

[12] P. Laleh, K. Yaser, O. Alireza, Oleoylethanolamide: A novel pharmaceutical agent in the management of obesity-an updated review, J. Cell. Physiol. 234 (6) (2019 Jun) 7893–7902, https://doi.org/10.1002/jcp.27913 (Epub 2018 Dec 7. PMID: 30537148).

[13] J. Brown, JD, Karimian Azari E, Ayala JE., Oleoylethanolamide: A fat ally in the fight against obesity, Physiol. Behav. 176 (2017 Jul 1) 50–58, https://doi.org/10.1016/j.physbeh.2017.02.034 (Epub 2017 Feb 27. PMID: 28254531).

[14] J. Sihag, P.J.H. Jones, Oleoylethanolamide: The role of a bioactive lipid amide in modulating eating behaviour, Obes. Rev. 19 (2) (2018 Feb) 178–197, https://doi.org/10.1111/obr.12630 (Epub 2017 Nov 10. PMID: 29124885).

[15] G.P. Ahern, Activation of TRPV1 by the satiety factor oleoylethanolamide, J. Biol. Chem. 278 (33) (2003 Aug 15) 30429–30434, https://doi.org/10.1074/jbc.M305051200 (Epub 2003 May 21. PMID: 12761211).

[16] J. Fu, F. Oveisi, S. Gaetani, E. Lin, D. Piomelli, Oleoylethanolamide, an endogenous PPAR-alpha agonist, lowers body weight and hyperlipidemia in obese rats, Neuropharmacology 48 (8) (2005 Jun) 1147–1153, https://doi.org/10.1016/j.neuropharm.2005.02.013 (Epub 2005 Apr 21. PMID: 15910890).

[17] T. Ren, A. Ma, R. Zhuo, H. Zhang, L. Peng, X. Jin, E. Yao, L. Yang, Oleoylethanolamide Increases Glycogen Synthesis and Inhibits Hepatic Gluconeogenesis via the LKB1/AMPK Pathway in Type 2 Diabetic Model, J. Pharmacol. Exp. Ther. 373 (1) (2020 Apr) 81–91, https://doi.org/10.1124/jpet.119.262675 (Epub 2020 Feb 5. PMID: 32024803).

[18] L. Yang, H. Guo, H. Li, X. Meng, L. Yan, Wu S. Dan Zhang, H. Zhou, L. Peng, Q. Xie, X. Jin, Oleoylethanolamide exerts anti-inflammatory effects on LPS-induced THP-1 cells by enhancing PPARα signaling and inhibiting the NF-κB and ERK1/2/AP-1/STAT3 pathways, Sci. Rep. 6 (2016 Oct 10) 34611, https://doi.org/10.1038/srep34611 (PMID: 27721381; PMCID: PMC5056375).

[19] J. Hu, Z. Zhu, H. Ying, J. Yao, H. Ma, L. Li, Y. Zhao, Oleoylethanolamide Protects Against Acute Liver Injury by Regulating Nrf-2/HO-1 and NLRP3 Pathways in Mice, Front. Pharmacol. 11 (2021 Jan 18) 605065, https://doi.org/10.3389/fphar.2020.605065 (PMID: 33536915; PMCID: PMC7848133).

[20] H. Tutunchi, A. Ostadrahimi, M. Saghafi-Asl, N. Roshanravan, A. Shakeri-Bavil, M. Asghari-Jafarabadi, N. Farrin, M. Mobasseri, Expression of NF-κB, IL-6, and IL-10 genes, body composition, and hepatic fibrosis in obese patients with NAFLD-Combined effects of oleoylethanolamide supplementation and calorie restriction: A triple-blind randomized controlled clinical trial, J. Cell. Physiol. 236 (1) (2021 Jan) 417–426, https://doi.org/10.1002/jcp.29870 (Epub 2020 Jun 22. PMID: 32572955).

[21] Y. Qin, J. Xie, R. Zheng, Y. Li, H. Wang, Oleoylethanolamide as a New Therapeutic Strategy to Alleviate Doxorubicin-Induced Cardiotoxicity, Front. Pharmacol. 13 (2022 Apr 20) 863322, https://doi.org/10.3389/fphar.2022.863322 (PMID: 35517792; PMCID: PMC9065409).

[22] M. Guzmán, J. Lo Verme, J. Fu, F. Oveisi, C. Blázquez, D. Piomelli, Oleoylethanolamide stimulates lipolysis by activating the nuclear receptor peroxisome proliferator-activated receptor alpha (PPAR-alpha), J. Biol. Chem. 279 (27) (2004 Jul 2) 27849–27854, https://doi.org/10.1074/jbc.M404087200 (Epub 2004 Apr 26. PMID: 15123613).

[23] Y. Qin, J. Xie, R. Zheng, Y. Li, H. Wang, Oleoylethanolamide as a New Therapeutic Strategy to Alleviate Doxorubicin-Induced Cardiotoxicity, Front. Pharmacol. 13 (2022 Apr 20) 863322, https://doi.org/10.3389/fphar.2022.863322 (PMID: 35517792; PMCID: PMC9065409).

[24] O.I. Voitychuk, V.S. Asmolkova, N.M. Gula, G.V. Sotkis, S. Galadari, F.C. Howarth, M. Oz, Y.M. Shuba, Modulation of excitability, membrane currents and survival of cardiac myocytes by N-acylethanolamines, Biochim. Biophys. Acta 1821 (9) (2012 Sep) 1167–1176, https://doi.org/10.1016/j.bbalip.2012.05.003 (Epub 2012 May 18. PMID: 22613942).

[25] M. Guzmán, J. Lo Verme, J. Fu, F. Oveisi, C. Blázquez, D. Piomelli, Oleoylethanolamide stimulates lipolysis by activating the nuclear receptor peroxisome proliferator-activated receptor alpha (PPAR-alpha), J. Biol. Chem. 279 (27) (2004 Jul 2) 27849–27854, https://doi.org/10.1074/jbc.M404087200 (Epub 2004 Apr 26. PMID: 15123613).

[26] P.L. Valenzuela, P. Carrera-Bastos, A. Castillo-García, D.E. Lieberman, A. Santos-Lozano, A. Lucia, Obesity and the risk of cardiometabolic diseases, Nat. Rev. Cardiol. 20 (7) (2023 Jul) 475–494, https://doi.org/10.1038/s41569-023-00847-5 (Epub 2023 Mar 16. PMID: 36927772).

[27] J. Barr, J. Caballería, I. Martínez-Arranz, A. Domínguez-Díez, C. Alonso, J. Muntané, M. Pérez-Cormenzana, C. García-Monzón, R. Mayo, A. Martín-Duce, M. Romero-Gómez, O. Lo Iacono, R.J. Andrade, M. Pérez-Carreras, Y. Le Marchand-Brustel, A. Tran, C. Fernández-Escalante, E. Arévalo, M. García-Unzueta, K. Clement, J. Crespo, P. Gual, M. Gómez-Fleitas, M.L. Martínez-Chantar, A. Castro, S.C. Lu, M. Vázquez-Chantada, J.M. Mato, Obesity-dependent metabolic signatures associated with nonalcoholic fatty liver disease progression, J. Proteome Res. 11 (4) (2012 Apr 6) 2521–2532, https://doi.org/10.1021/pr201223p (Epub 2012 Mar 15. PMID: 22364559; PMCID: PMC3321123).

[28] W.C. Claycomb, N.A. Lanson Jr., B.S. Stallworth, D.B. Egeland, J.B. Delcarpio, A. Bahinski, N.J. Izzo Jr., HL-1 cells: a cardiac muscle cell line that contracts and retains phenotypic characteristics of the adult cardiomyocyte, Proc. Natl. Acad. Sci. U. S. A. 95 (6) (1998 Mar 17) 2979–2984, https://doi.org/10.1073/pnas.95.6.2979 (PMID: 9501201; PMCID: PMC19680).

[29] I. Martínez-Arranz, R. Mayo, M. Pérez-Cormenzana, I. Mincholé, L. Salazar, C. Alonso, J.M. Mato, Enhancing metabolomics research through data mining, J. Proteomics 127 (Pt B) (2015 Feb 7) 275–288, https://doi.org/10.1016/j.jprot.2015.01.019 (Epub 2015 Feb 7. PMID: 25668325).

[30] A. Jovanovic, B. Xu, C. Zhu, D. Ren, H. Wang, M. Krause-Hauch, E.D. Abel, J. Li, Y. K. Xiang, Characterizing Adrenergic Regulation of Glucose Transporter 4-Mediated Glucose Uptake and Metabolism in the Heart, JACC Basic Transl Sci. 8 (6) (2023 Feb 22) 638–655, https://doi.org/10.1016/j.jacbts.2022.11.008 (PMID: 37426525; PMCID: PMC10322917).

[31] X. Chen, A. Sun, Y. Zou, J. Ge, J.M. Lazar, X.C. Jiang, Impact of sphingomyelin levels on coronary heart disease and left ventricular systolic function in humans, Nutr. Metab. (Lond.) 8 (1) (2011 Apr 26) 25, https://doi.org/10.1186/1743-7075-8-25 (PMID: 21521522; PMCID: PMC3111338).

[32] X. Zhang, J. Fan, H. Li, C. Chen, Y. Wang, CD36 Signaling in Diabetic Cardiomyopathy, Aging Dis. 12 (3) (2021 Jun 1) 826–840, https://doi.org/10.14336/AD.2020.1217 (PMID: 34094645; PMCID: PMC8139204).

[33] F. Ge, C. Hu, E. Hyodo, K. Arai, S. Zhou, H. Lobdell 4th, J.L. Walewski, S. Homma, P.D. Berk, Cardiomyocyte triglyceride accumulation and reduced ventricular function in mice with obesity reflect increased long chain Fatty Acid uptake and de novo Fatty Acid synthesis, J. Obes. 2012 (2012) 205648, https://doi.org/10.1155/2012/205648 (Epub 2011 Nov 2. PMID: 22132320; PMCID: PMC3216284).

[34] F.M. Campbell, R. Kozak, A. Wagner, J.Y. Altarejos, J.R. Dyck, D.D. Belke, D. L. Severson, D.P. Kelly, G.D. Lopaschuk, A role for peroxisome proliferator-activated receptor alpha (PPARalpha) in the control of cardiac malonyl-CoA levels: reduced fatty acid oxidation rates and increased glucose oxidation rates in the hearts of mice lacking PPARalpha are associated with higher concentrations of malonyl-CoA and reduced expression of malonyl-CoA decarboxylase, J. Biol. Chem. 277 (6) (2002 Feb 8) 4098–4103, https://doi.org/10.1074/jbc.M106054200 (Epub 2001 Dec 4. PMID: 11734553).

[35] W.S. Lee, J. Kim, Peroxisome Proliferator-Activated Receptors and the Heart: Lessons from the Past and Future Directions, PPAR Res. 2015 (2015) 271983, https://doi.org/10.1155/2015/271983 (Epub 2015 Oct 26. PMID: 26587015; PMCID: PMC4637490).

[36] J.C. Fraulob, R. Ogg-Diamantino, C. Fernandes-Santos, M.B. Aguila, C. A. Mandarim-de-Lacerda, A Mouse Model of Metabolic Syndrome: Insulin Resistance, Fatty Liver and Non-Alcoholic Fatty Pancreas Disease (NAFPD) in C57BL/6 Mice Fed a High Fat Diet, J. Clin. Biochem. Nutr. 46 (3) (2010 May) 212–223, https://doi.org/10.3164/jcbn.09-83 (Epub 2010 Apr 10. PMID: 20490316; PMCID: PMC2872226).

[37] M.C. Della Vedova, M.D. Muñoz, L.D. Santillan, M.G. Plateo-Pignatari, M. J. Germanó, M.E. Rinaldi Tosi, S. Garcia, N.N. Gomez, M.W. Fornes, S.E. Gomez Mejiba, D.C. Ramirez, A Mouse Model of Diet-Induced Obesity Resembling Most Features of Human Metabolic Syndrome, Nutr Metab Insights. 9 (2016 Dec 5) 93–102, https://doi.org/10.4137/NMI.S32907 (PMID: 27980421; PMCID: PMC5140012).

[38] X.A. Wang, R. Zhang, S. Zhang, S. Deng, D. Jiang, J. Zhong, L. Yang, T. Wang, S. Hong, S. Guo, Z.G. She, X.D. Zhang, H. Li, Interferon regulatory factor 7 deficiency prevents diet-induced obesity and insulin resistance, Am. J. Physiol. Endocrinol. Metab. 305 (4) (2013 Aug 15) E485–E495, https://doi.org/10.1152/ajpendo.00505.2012 (Epub 2013 May 21. PMID: 23695216).

[39] E.D. Abel, S.E. Litwin, G. Sweeney, Cardiac remodeling in obesity, Physiol. Rev. 88 (2) (2008 Apr) 389–419, https://doi.org/10.1152/physrev.00017.2007 (PMID: 18391168; PMCID: PMC2915933).

[40] S. Tiwari, J.F. Ndisang, The role of obesity in cardiomyopathy and nephropathy, Curr. Pharm. Des. 20 (9) (2014) 1409–1417, https://doi.org/10.2174/13816128113199990562 (PMID: 23978095).

[41] I.P. Salt, D.G. Hardie, AMP-Activated Protein Kinase: An Ubiquitous Signaling Pathway With Key Roles in the Cardiovascular System, Circ. Res. 120 (11) (2017

[42] R.R. Russell 3rd, R. Bergeron, G.I. Shulman, L.H. Young, Translocation of myocardial GLUT-4 and increased glucose uptake through activation of AMPK by AICAR, Am. J. Physiol. 277 (2) (1999 Aug) H643–H649, https://doi.org/10.1152/ajpheart.1999.277.2.H643 (PMID: 10444490).

[43] H.F. Kramer, C.A. Witczak, N. Fujii, N. Jessen, E.B. Taylor, D.E. Arnolds, K. Sakamoto, M.F. Hirshman, L.J. Goodyear, Distinct signals regulate AS160 phosphorylation in response to insulin, AICAR, and contraction in mouse skeletal muscle, Diabetes 55 (7) (2006 Jul) 2067–2076, https://doi.org/10.2337/db06-0150 (PMID: 16804077).

[44] A. Ginion, J. Auquier, C.R. Benton, C. Mouton, J.L. Vanoverschelde, L. Hue, S. Horman, C. Beauloye, L. Bertrand, Inhibition of the mTOR/p70S6K pathway is not involved in the insulin-sensitizing effect of AMPK on cardiac glucose uptake, Am. J. Physiol. Heart Circ. Physiol. 301 (2) (2011 Aug) H469–H477, https://doi.org/10.1152/ajpheart.00986.2010 (Epub 2011 May 20. PMID: 21602475).

[45] P. Heim, C. Morandi, G.R. Brouwer, L. Xu, C. Montessuit, M. Brink, Neuregulin-1 triggers GLUT4 translocation and enhances glucose uptake independently of insulin receptor substrate and ErbB3 in neonatal rat cardiomyocytes. Biochim Biophys Acta Mol, Cell Res. 1867 (3) (2020 Mar) 118562, https://doi.org/10.1016/j.bbamcr.2019.118562 (Epub 2019 Oct 25. PMID: 31669265).

[46] S. Shoop, Z. Maria, A. Campolo, N. Rashdan, D. Martin, P. Lovern, V.A. Lacombe, Glial Growth Factor 2 Regulates Glucose Transport in Healthy Cardiac Myocytes and During Myocardial Infarction via an Akt-Dependent Pathway, Front. Physiol. 10 (2019 Mar 27) 189, https://doi.org/10.3389/fphys.2019.00189 (PMID: 30971932; PMCID: PMC6445869).

[47] S. Feijóo-Bandín, D. Rodríguez-Penas, V. García-Rúa, A. Mosquera-Leal, M. F. Otero, E. Pereira, J. Rubio, I. Martínez, L.M. Seoane, O. Gualillo, M. Calaza, T. García-Caballero, M. Portolés, E. Roselló-Lletí, C. Diéguez, M. Rivera, J. R. González-Juanatey, F. Lago, Nesfatin-1 in human and murine cardiomyocytes: synthesis, secretion, and mobilization of GLUT-4, Endocrinology 154 (12) (2013 Dec) 4757–4767, https://doi.org/10.1210/en.2013-1497 (Epub 2013 Sep 24. PMID: 24064358).

[48] E. Dirkx, R.W. Schwenk, J.F. Glatz, J.J. Luiken, G.J. van Eys, High fat diet induced diabetic cardiomyopathy, Prostaglandins Leukot. Essent. Fatty Acids 85 (5) (2011 Nov) 219–225, https://doi.org/10.1016/j.plefa.2011.04.018 (Epub 2011 May 14. PMID: 21571515).

[49] J.F.C. Glatz, J.J.F.P. Luiken, M. Nabben, CD36 (SR-B2) as a Target to Treat Lipid Overload-Induced Cardiac Dysfunction, J Lipid Atheroscler 9 (1) (2020 Jan) 66–78, https://doi.org/10.12997/jla.2020.9.1.66 (Epub 2020 Jan 8. PMID: 32821722; PMCID: PMC7379071).

[50] F. Ge, C. Hu, E. Hyodo, K. Arai, S. Zhou, H. Lobdell 4th, J.L. Walewski, S. Homma, P.D. Berk, Cardiomyocyte triglyceride accumulation and reduced ventricular function in mice with obesity reflect increased long chain Fatty Acid uptake and de novo Fatty Acid synthesis, J Obes 2012 (2012) 205648, https://doi.org/10.1155/2012/205648 (Epub 2011 Nov 2. PMID: 22132320; PMCID: PMC3216284).

[51] B. Zhang, X. Li, G. Liu, C. Zhang, X. Zhang, Q. Shen, G. Sun, X. Sun, Peroxiredoxin-4 ameliorates lipotoxicity-induced oxidative stress and apoptosis in diabetic cardiomyopathy, Biomed. Pharmacother. 141 (2021 Sep) 111780, https://doi.org/10.1016/j.biopha.2021.111780 (Epub 2021 Jun 12. PMID: 34130124).

[52] H. Shu, Y. Peng, W. Hang, J. Nie, N. Zhou, D.W. Wang, The role of CD36 in cardiovascular disease, Cardiovasc. Res. 118 (1) (2022 Jan 7) 115–129, https://doi.org/10.1093/cvr/cvaa319 (PMID: 33210138; PMCID: PMC8752351).

[53] G. Nanayakkara, T. Kariharan, L. Wang, J. Zhong, R. Amin, The cardio-protective signaling and mechanisms of adiponectin, Am J Cardiovasc Dis 2 (4) (2012) 253–266 (Epub 2012 Oct 20. PMID: 23173099; PMCID: PMC3499932).

[54] S.L. Zheng, Z.Y. Li, J. Song, J.M. Liu, C.Y. Miao, Metrnl: a secreted protein with new emerging functions, Acta Pharmacol. Sin. 37 (5) (2016 May) 571–579, https://doi.org/10.1038/aps.2016.9 (Epub 2016 Apr 11. PMID: 27063217; PMCID: PMC4857552).

[55] L. Sojo, E. Santos-González, L. Riera, A. Aguilera, R. Barahona, P. Pellicer, M. Buxó, J. Mayneris-Perxachs, M. Fernandez-Balsells, J.M. Fernández-Real, Plasma Lipidomics Profiles Highlight the Associations of the Dual Antioxidant/Pro-oxidant Molecules Sphingomyelin and Phosphatidylcholine with Subclinical Atherosclerosis in Patients with Type 1 Diabetes, Antioxidants (Basel) M12 (5) (2023 May 20) 1132, https://doi.org/10.3390/antiox12051132 (PMID: 37237999; PMCID: PMC10215275).

[56] G. Pepe, M. Cotugno, F. Marracino, L. Capocci, L. Pizzati, M. Forte, R. Stanzione, P. Scarselli, Ai Di Pardo, S. Sciarretta, M. Volpe, S. Rubattu, V. Maglione, Abnormal expression of sphingolipid-metabolizing enzymes in the heart of spontaneously hypertensive rat models, Biochim Biophys Acta Mol Cell Biol Lipids 1869 (1) (2024 Jan) 159411, https://doi.org/10.1016/j.bbalip.2023.159411 (Epub 2023 Nov 9. PMID: 37949293).

[57] R. Liu, T. Duan, L. Yu, Y. Tang, S. Liu, C. Wang, W.J. Fang, Acid sphingomyelinase promotes diabetic cardiomyopathy via NADPH oxidase 4 mediated apoptosis, Cardiovasc. Diabetol. 22 (1) (2023 Feb 2) 25, https://doi.org/10.1186/s12933-023-01747-1 (PMID: 36732747; PMCID: PMC9896821).

[58] M. Bujak, G. Ren, H.J. Kweon, M. Dobaczewski, A. Reddy, G. Taffet, X.F. Wang, N. G. Frangogiannis, Essential role of Smad3 in infarct healing and in the pathogenesis of cardiac remodeling, Circulation 116 (19) (2007 Nov 6) 2127–2138, https://doi.org/10.1161/CIRCULATIONAHA.107.704197 (Epub 2007 Oct 22. PMID: 17967775).

[59] T.P. Thomas, L.A. Grisanti, The Dynamic Interplay Between Cardiac Inflammation and Fibrosis, Front. Physiol. 11 (2020 Sep 15) 529075, https://doi.org/10.3389/fphys.2020.529075 (PMID: 33041853; PMCID: PMC7522448).

May 26) 1825–1841, https://doi.org/10.1161/CIRCRESAHA.117.309633 (PMID: 28546359; PMCID: PMC5447810).

[60] N.G. Frangogiannis, Cardiac fibrosis, Cardiovasc. Res. 117 (6) (2021 May 25) 1450–1488, https://doi.org/10.1093/cvr/cvaa324. PMID: 33135058; PMCID: PMC8152700.

[61] J. Kruszewska, A. Cudnoch-Jedrzejewska, K. Czarzasta, Remodeling and Fibrosis of the Cardiac Muscle in the Course of Obesity-Pathogenesis and Involvement of the Extracellular Matrix, Int. J. Mol. Sci. 23 (8) (2022 Apr 11) 4195, https://doi.org/10.3390/ijms23084195 (PMID: 35457013; PMCID: PMC9032681).

[62] A. Terman, U.T. Brunk, Autophagy in cardiac myocyte homeostasis, aging, and pathology, Cardiovasc. Res. 68 (3) (2005 Dec 1) 355–365, https://doi.org/10.1016/j.cardiores.2005.08.014 (Epub 2005 Oct 6. PMID: 16213475).

[63] Y. Kabeya, N. Mizushima, T. Ueno, A. Yamamoto, T. Kirisako, T. Noda, E. Kominami, Y. Ohsumi, T. Yoshimori, LC3, a mammalian homologue of yeast Apg8p, is localized in autophagosome membranes after processing, EMBO J. 19 (21) (2000 Nov 1) 5720–5728, https://doi.org/10.1093/emboj/19.21.5720 (Erratum in: EMBO J. 2003 Sep 1;22(17):4577. PMID: 11060023; PMCID: PMC305793).

[64] L. Esteban-Martínez, P. Boya, Autophagic flux determination in vivo and ex vivo, Methods 75 (2015 Mar) 79–86, https://doi.org/10.1016/j.ymeth.2015.01.008 (Epub 2015 Jan 30. PMID: 25644445).

[65] Y. Katsuragi, Y. Ichimura, M. Komatsu, p62/SQSTM1 functions as a signaling hub and an autophagy adaptor, FEBS J. 282 (24) (2015 Dec) 4672–4678, https://doi.org/10.1111/febs.13540 (Epub 2015 Oct 16. PMID: 26432171).

[66] R. Kumari, A.G. Ray, D. Mukherjee, V. Chander, D. Kar, U.S. Kumar, P.V.P. D. Bharadwaj, S.K. Banerjee, A. Konar, A. Bandyopadhyay, Downregulation of PTEN Promotes Autophagy *via* Concurrent Reduction in Apoptosis in Cardiac Hypertrophy in PPAR α$^{-/-}$ Mice, Front Cardiovasc Med. 9 (2022 Feb 11) 798639, https://doi.org/10.3389/fcvm.2022.798639 (PMID: 35224041; PMCID: PMC8881053).

[67] J. Yan, K. Song, Z. Bai, R.L. Ge, WY14643 improves left ventricular myocardial mitochondrial and systolic functions in obese rats under chronic persistent hypoxia via the PPARα pathway, Life Sci. 266 (2021 Feb 1) 118888, https://doi.org/10.1016/j.lfs.2020.118888 (Epub 2020 Dec 10. PMID: 33310031).

[68] I.R. Schlaepfer, M. Joshi, CPT1A-mediated Fat Oxidation, Mechanisms, and Therapeutic Potential, Endocrinology 161 (2) (2020 Feb 1) bqz046, https://doi.org/10.1210/endocr/bqz046. 31900483.

[69] K. Watanabe, H. Fujii, T. Takahashi, M. Kodama, Y. Aizawa, Y. Ohta, T. Ono, G. Hasegawa, M. Naito, T. Nakajima, Y. Kamijo, F.J. Gonzalez, T. Aoyama, Constitutive regulation of cardiac fatty acid metabolism through peroxisome proliferator-activated receptor alpha associated with age-dependent cardiac toxicity, J. Biol. Chem. 275 (29) (2000 Jul 21) 22293–22299, https://doi.org/10.1074/jbc.M000248200 (PMID: 10801788).

[70] J.E. Zarrow, A.M. Alli-Oluwafuyi, C.M. Youwakim, K. Kim, A.N. Jenkins, I. C. Suero, M.R. Jones, Z. Mashhadi, K. Mackie, A.G. Waterson, A.C. Doran, G. A. Sulikowski, S.S. Davies, Small Molecule Activation of NAPE-PLD Enhances Efferocytosis by Macrophages, ACS Chem. Biol. 18 (8) (2023 Aug 18) 1891–1904, https://doi.org/10.1021/acschembio.3c00401 (Epub 2023 Aug 2. PMID: 37531659; PMCID: PMC10443532).

[71] P. Rinne, R. Guillamat-Prats, M. Rami, L. Bindila, L. Ring, L.P. Lyytikäinen, E. Raitoharju, N. Oksala, T. Lehtimäki, C. Weber, E.P.C. van der Vorst, S. Steffens, Palmitoylethanolamide Promotes a Proresolving Macrophage Phenotype and Attenuates Atherosclerotic Plaque Formation, Arterioscler. Thromb. Vasc. Biol. 38 (11) (2018 Nov) 2562–2575, https://doi.org/10.1161/ATVBAHA.118.311185 (PMID: 30354245).

[72] R. Di Paola, R. Fusco, E. Gugliandolo, R. D'Amico, M. Campolo, S. Latteri, A. Carughi, G. Mandalari, S. Cuzzocrea, The Antioxidant Activity of Pistachios Reduces Cardiac Tissue Injury of Acute Ischemia/Reperfusion (I/R) in Diabetic Streptozotocin (STZ)-Induced Hyperglycaemic Rats, Front. Pharmacol. 9 (2018 Feb 6) 51, https://doi.org/10.3389/fphar.2018.00051 (PMID: 29467653; PMCID: PMC5808141).

[73] P. Lépicier, J.F. Bouchard, C. Lagneux, D. Lamontagne, Endocannabinoids protect the rat isolated heart against ischaemia, Br. J. Pharmacol. 139 (4) (2003 Jun) 805–815, https://doi.org/10.1038/sj.bjp.0705313 (PMID: 12813004; PMCID: PMC1573907).

[74] G. Mattace Raso, C. Pirozzi, d'Emmanuele di Villa, R. Bianca, R. Simeoli, A. Santoro, A. Lama, F. Di Guida, R. Russo, C. De Caro, R. Sorrentino, A. Calignano, R. Meli, Palmitoylethanolamide treatment reduces blood pressure in spontaneously hypertensive rats: involvement of cytochrome p450-derived eicosanoids and renin angiotensin system, PLoS One 10 (5) (2015 May 7) e0123602, https://doi.org/10.1371/journal.pone.0123602 (PMID: 25951330; PMCID: PMC4423982).

[75] Y. Pu, C.K. Cheng, H. Zhang, J.Y. Luo, L. Wang, B. Tomlinson, Y. Huang, Molecular mechanisms and therapeutic perspectives of peroxisome proliferator-activated receptor α agonists in cardiovascular health and disease, Med. Res. Rev. 43 (6) (2023 Nov) 2086–2114, https://doi.org/10.1002/med.21970 (Epub 2023 Apr 29. PMID: 37119045).

[76] L. Wang, Y. Cai, L. Jian, C.W. Cheung, L. Zhang, Z. Xia, Impact of peroxisome proliferator-activated receptor-α on diabetic cardiomyopathy, Cardiovasc. Diabetol. 20 (1) (2021 Jan 4) 2, https://doi.org/10.1186/s12933-020-01188-0 (PMID: 33397369; PMCID: PMC7783984).